Growth Analysis of Interfacial Delamination of Plastic Ball Grid Array Package During Solder Reflow

Kuo-Chin Chang[1] **and Kuo-Ning Chiang**[2]

Abstract

This work investigated the initial location of the possible delamination in a PBGA package under moisture preconditioning and subsequent solder reflow by applying the modified Tsai-Hill failure criteria. The fracture parameters such as the stress intensity factor, the strain energy release rate, and the phase angle at the delamination tip, were calculated to study delamination growth. A 2-D PBGA model was considered and the hygrothermal stress at interfaces was calculated to examine the initiation of delamination. A 3-D PBGA model was applied in the study of delamination growth. A global-local finite element analysis and 2-D linear interfacial fracture mechanics were used to calculate fracture parameters at the delaminaton tip for different delamination lengths. The effect of vaporized moisture inside the PBGA package on the growing delamination was examined. A series of popcorn experiments on PBGA packages were carried out to verify the simulation results. The agreement between the predicted and experimental results was good.

Keywords: Solder Reflow, Fracture Parameters, Delamination Growth, Global-Local Finite Element Analysis, 2-D Linear Interfacial Fracture Mechanics

---

[1] Ph. D. Student, Department of Power Mechanical Engineering, National Tsing Hua University, Hsinchu 300, Taiwan.
[2] Associate Professor, Department of Power Mechanical Engineering, National Tsing Hua University, Hsinchu 300, Taiwan.
Corresponding Author

1 Introduction

The PBGA package will simultaneously absorb the moisture and permeate inwards under humid and hot conditions for an extended period. The absorbed moisture can decrease the adhesion at interfaces [Nguyen (1993); Hawkins, Ganesan, Lewis, and Berg (1995)]. When the PBGA package undergoes the early stage of the solder reflow process, initial delamination at some specific locations of already weakened interfaces may be induced due to mismatch among the coefficients of thermal expansion (CTE) among the packaging components. Then, the absorbed moisture diffuses into the delamination areas and turns into steam, generating additional pressure acting upon the crack surfaces. If the strain energy release rate generated by the loads (hygrothermal stress and steam pressure) exceeds the interfacial fracture toughness, delaminations will propagate and possibly lead to popcorn cracking.

Earlier studies [Ahn, and Kwon (1995); Hawkins, Ganesan, Lewis, and Berg (1995); Yeh and Chang (1999a)] revealed that the initial delaminations in the PBGA package are usually detected at die attach or die pad corners during moisture preconditioning and solder reflow. Delaminations further propagate in the inward and outward directions along weak interfaces such as the die attach/die pad interface, the EMC/die pad interface, etc., or through materials with low fracture toughness. Delamination is an important damage mode and can degrade the long term operating reliability of the PBGA package. Therefore, it is important to find the locations of initial delamination, and understand how it would behave at interfaces during reflowing.

Herein, the entire moisture and thermal simulation of the PBGA package runs from moisture preconditioning to the solder reflow process. First, the hygrothermal stress in the PBGA package under the solder reflow was calculated, and the regions of higher stress, especially at interfaces, were examined. The initiation of interfacial delamination can be predicted by applying the failure criteria. The fracture parameters such as the stress intensity factor, the strain energy release rate, and the phase angle at the delamination tip for different delamination lengths, were then calculated using a global-local finite element analysis and 2-D linear interfacial fracture mechanics, to study the growth of initial delamination. The effect of vaporized moisture inside the PBGA package on delamination growth was examined. Experimentally, the moisture absorption and diffusion of the PBGA package was carried out in an hygrothermal chamber and the solder reflow process was simulated in a reflow oven. The PBGA package was inspected using an ultrasonic C-mode scanning system before and after the hygrothermal test to examine its delamination or popcorn cracking.

2 Analysis

The analysis in the present study considers (a) heat transfer (b) moisture diffusion (c) hygrothermal stress (d) failure criteria (e) global-local finite element analysis and (f) interfacial fracture mechanics as they apply to the deformation and damage of the PBGA package. Detailed simulations of moisture diffusion during moisture preconditioning and solder reflow and the hygrothermal stress analysis during solder reflow are described by Chang, Yeh, and Chiang. The interfaces in the PBGA package are checked for failure according to the failure criteria after the hygrothermal stress is calculated.

2.1 Failure criteria

For a PBGA package, the failures at interfaces are mainly determined from the peeling stress σ_y and the shear stress τ_{xy}. The Tsai-Hill failure criteria can be properly modified as [Mei and Liu (1995)]

$$\sqrt{\left(\frac{\sigma_y}{\sigma_y^f}\right)^2+\left(\frac{\tau_{xy}}{\tau_{xy}^f}\right)^2}=f_d \tag{1}$$

where $\sigma^f{}_y$ is the critical peeling stress, $\tau^f{}_{xy}$ is the critical shear stress, and f_d is the failure index. The interfaces fail when $f_d \geqq 1$.

2.2 Global-local finite element analysis

Herein, global-local finite element analysis was applied to the 3-D PBGA model with delamination for reducing the number of elements in the mesh model and the total solution time. The specified boundary method (SBM) was used for performing the global-local analysis, which involves the following stages [Voleti, Chandra, and Miller (1996)].

(1) Creating the global and local meshes. In the present study, the global mesh refers to the mesh that models the 3-D PBGA structure with delamination. The local mesh was created for calculating the fracture parameters at the delamination tip using 2-D linear interfacial fracture mechanics. The local mesh models the symmetric area close to the delamination tip and is more detailed than the global mesh because the 2-D delamination mechanics refers to the plane strain case and the symmetric cross-section of the PBGA package has no out-of-plane displacements.

(2) Extracting and interpolating nodal displacements at the global-local boundary. Nodal data must be interpolated from the global mesh solution because the global mesh has fewer nodes than the local mesh at the global-local boundary. Extracting and interpolating the nodal displacements of the global model gives the nodal displacements at the boundary of the local mesh.

(3) Analyzing the local problem. The interpolated nodal displacements constitute the boundary condition

of the local problem. The tendency of interfacial delamination to grow is studied at this stage.

2.3 Interfacial fracture Mechanics analysis

The interfacial delamination in the PBGA package has mixed-mode fracture characteristics, due to the combined effects of the CTE mismatch between materials and the applied steam pressure. These modes are the opening mode I and the shearing mode II. The stress intensity factor (SIF) at a bimaterial (say material 1 and material 2) interface crack tip can be measured from the crack tip opening displacements (CTOD), u_x and u_y. See Fig. 1. According to Saitoh, Matsuyama, and Toya (1998), the relationship between SIF at the crack tip and CTOD can be expressed as follows.

$$\begin{aligned} K_I = C \lim_{r\to 0}[u_y(\cos Q + 2\omega \sin Q) \\ + u_x(\sin Q - 2\omega \cos Q)] / \sqrt{r/2\pi} \end{aligned} \tag{2}$$

$$\begin{aligned} K_{II} = C \lim_{r\to 0}[u_x(\cos Q + 2\omega \sin Q) \\ - u_y(\sin Q - 2\omega \cos Q)] / \sqrt{r/2\pi} \end{aligned} \tag{3}$$

where

$$\omega = \frac{1}{2\pi} \ln\left[\left(\frac{\kappa_1}{\mu_1} + \frac{1}{\mu_2}\right) \bigg/ \left(\frac{\kappa_2}{\mu_2} + \frac{1}{\mu_1}\right)\right] \tag{4}$$

$$C = 2\cosh(\omega\pi) / [\,(\kappa_1 + 1)/\mu_1 + (\kappa_2 + 1)/\mu_2\,] \tag{5}$$

$$Q = \omega \ln(r/L) \tag{6}$$

where K_I and K_{II} are the SIF corresponding to mode I and mode II, respectively; r is the distance from the crack tip, and κ_j=3-4ν_j (j=1,2) for plane strain cases. ν and μ are the Poisson's ratio and shear modulus, respectively, and the subscripts (1 and 2) indicate the corresponding materials. ω denotes the effective property of materials in the neighborhood of the crack tip. L is a characteristic length introduced by Rice (1988), that causes the dimensions of K_I and K_{II} for bimaterial system to be the same as that for homogeneous solids. Rice (1988) pointed out that Eqs. 2 and 3 can be used only when r/L<0.01. In this paper, L=0.25mm and the range r=0.001mm~0.025mm was adopted. Subsequently, the effective SIF, K_{eff}, the phase angle ψ and the strain energy release rate G at the crack tip can be obtained as

$$K_{eff} = \sqrt{K_I^2 + K_{II}^2} \tag{7}$$

$$G = \frac{1}{16\cosh^2(\omega\pi)}\left[\frac{\kappa_1+1}{\mu_1} + \frac{\kappa_2+1}{\mu_2}\right](K_I^2 + K_{II}^2) \tag{8}$$

$$\psi = \tan^{-1}\left(\frac{K_{II}}{K_I}\right) \tag{9}$$

The phase angle is an index which defines the dominance of mixed-mode fracture (for opening mode I, ψ<45degrees and for shearing mode II, ψ>45degrees).

The condition for further delamination propagation along the interface is

$$G = \Gamma \tag{10}$$

where Γ is the interface fracture toughness assumed to be a function of the phase angle ψ [Hutchinson and Suo (1991)].

$$\Gamma(\psi) = \Gamma_I^c[1 + (1-\lambda)\tan^2\psi] \tag{11}$$

where Γ_I^c is the interfacial fracture toughness at the opening mode I and λ is a fitting constant. Park and Yu (1997) proposed λ=0.5 be taken in the interfacial delamination of plastic IC packages.

Lau and Lee (2000) proposed another computational method for obtaining the fracture parameters from CTOD. This method is also used in this study and compared with that defined by Saitoh, Matsuyama, and Toya (1998). According to Lau and Lee (2000), the relationship between SIF (K_I and K_{II}) and CTOD can be expressed as follows.

$$\begin{aligned} K_I = {} & [(u_y - 2\varepsilon u_x)\cos(\varepsilon \ln r) \\ & + (u_x + 2\varepsilon u_y)\sin(\varepsilon \ln r)]/D \end{aligned} \tag{12}$$

$$\begin{aligned} K_{II} = {} & [(u_x + 2\varepsilon u_y)\cos(\varepsilon \ln r) \\ & - (u_y - 2\varepsilon u_x)\sin(\varepsilon \ln r)]/D \end{aligned} \tag{13}$$

where

$$\varepsilon = \frac{1}{2\pi}\ln\left(\frac{1-\beta}{1+\beta}\right) \tag{14}$$

$$D = \frac{4}{\cosh(\varepsilon\pi)}\frac{E_1 + E_2}{E_1 E_2}\left(\frac{r}{2\pi}\right)^{1/2} \tag{15}$$

E is the elastic modulus and the subscripts (1 and 2) indicate the corresponding materials. For the plane strain case,

$$\beta = \frac{1}{2}\frac{\mu_1(1-2\nu_2)-\mu_2(1-2\nu_1)}{\mu_1(1-\nu_2)+\mu_2(1-\nu_1)} \tag{16}$$

the strain energy release rate G can be obtained as

$$G = \frac{1}{2}(1-\beta^2)\frac{E_1+E_2}{E_1E_2}(K_I^2+K_{II}^2) \tag{17}$$

3 Results and discussion

The PBGA package with 256 I/O's of 1.27-mm pitch was analyzed by the finite element method to simulate the moisture absorption and subsequent solder reflow processes. Fig. 2 shows top and bottom views of the PBGA package. The moisture absorption simulation refers to the JEDEC (1995) level 1 moisture test standard. The PBGA package was placed in a chamber at 85℃/85% RH for 168 hours. The solder reflow simulation refers to the JEDEC (1995) Infrared (IR) solder reflow test standard and the peak reflow temperature is 220℃. The initial states inside the PBGA package are taken to be such that the moisture content is zero and the stress-free temperature is 25℃. No internal heat source inside the PBGA package is generated in the analysis. Tab. 1 lists the material properties of the PBGA package used in this present simulation, in which x, y and z are Cartesian coordinates with the xy plane as the cross section of PBGA package.

3.1 Detecting delamination initiation

The induced hygrothermal stresses (mainly the peeling and shear stresses) at EMC/die, die/die attach and EMC/die pad interfaces of the PBGA package were calculated for a temperature of 220℃ during the solder reflow process. The initiation of interfacial delamination can be predicted by applying the failure criteria. Tab. 2 displays the allowable peeling and shear stresses at EMC/die, die /die attach and EMC/die pad interfaces. In this part, a 2-D PBGA model was created. Only the right half of the PBGA package is analyzed due to symmetry. Fig. 3 displays the cross-sectional dimensions of the PBGA package. The hygrothermal stresses of the PBGA package were calculated using the finite element method involving an eight-node plane element with two degrees of freedom. Fig. 4 shows analytical hygrothermal peeling and shear stresses at the EMC/die pad interface. According to the failure criteria and Tab. 2, delamination initiation is expected at the EMC/die pad interface near the corners of the die and die pad, since $f_d > 1$ (as shown in Fig. 5). Tab. 3 lists the maximum failure index f_d at other interfaces. This table shows that the EMC/die and die/die attach interfaces do not fail due to peeling and shear stresses, since $f_d < 1$.

3.2 Growth of initial delamination

During the reflowing, the moisture inside the PBGA package is assumed to evaporate, and the steam pressure is assumed to act on the surfaces of delamination. In the present study, the steam pressure P(T) can be estimated using the following equation [Shirley and McCullen (1995)].

$$P(T) = P_0 \exp\left[4640\left(\frac{1}{358} - \frac{1}{T}\right)\right] \quad (18)$$

where P_0 is a constant (0.049 MPa) and T is the reflow temperature (K). When the reflow temperature T reaches 220℃ (the temperature considered in this work), the steam pressure inside the delamination of the PBGA package is estimated to be about 1.71 MPa according to Eq. 18. During the reflowing, both thermal stress and steam pressure loadings affect the tendency of initial delamination to grow. The steam pressure loading is generally considered to contribute to the opening mode I while the thermal stress loading mainly contributes to the shearing mode II. Delaminated PBGA packages both with and without moisture were analyzed in this paper to study the effect of steam pressure on the growth of initial delamination.

- *Assumptions of delamination models*

The delamination was assumed to be initiated at the EMC/die pad interface near the corner of the die pad. It was assumed that the crack started to propagate along the top surface of the die pad toward the center of the die attach/die pad interface after delamination was initiated, as shown in Fig. 5. The initial delamination length d was varied in five steps: 0.5, 1.0, 2.5, 3.5 and 4 mm, to study the growth tendency of different initial delamination lengths.

Fig. 6 shows the one-eighth finite element mesh of the 3-D PBGA package with delamination used in the growth analysis of initial delamination. The three-dimensional finite element mesh does not include the solder balls for computational efficiency since the solder balls do not influence the interfacial stress distribution of the PBGA package [Yeh and Chang (1999b)]. The eight-node brick element with three degrees of freedom was used in the hygrothermal stress analysis. The global PBGA analysis aims to obtain the nodal displacements at the boundary of the detailed local analysis. Fig. 7 shows the finite element local mesh near the delamination tip on the symmetric area of the PBGA package. The six-node triangle element with two degrees of freedom was used in the interfacial fracture analysis. The range of element edge length close to the delamination tip is about 1μm~10μm, small enough for necessary precision of the analytical results.

- ***Growth of interfacial delamination in the PBGA package without moisture***

Fig. 8 shows the stress intensity factors and the phase angle (calculated from Eqs. 2, 3 and 9) at the delamination tip of the PBGA package without moisture, for different delamination lengths at 220℃. Fig. 8 indicates that K_{II} initially increases with the delamination length d, reaches a maximum at d=2.5 mm, and then gradually decreases to a stable value for d>2.5 mm. K_{II} nearly equals K_{eff} and the phase angle ψ exceeds 60 degrees for all delamination lengths. Hence, for the case of the PBGA package without moisture, shear mode II dominates the fracture mode in the growth of delamination. This is a direct result under thermal loading due to the thermal expansion mismatch among materials,

Fig. 9 and Tab. 4 display the strain energy release rate (calculated from Eqs. 8 and 17) and the normalized fracture toughness Γ/Γ_I^c (calculated from Eq. 11) at the delamination tip of the PBGA package without moisture, for different delamination lengths at 220℃. The maximum difference between G calculated by the method proposed by Saitoh, Matsuyama, and Toya (1998) and G calculated by that proposed by Lau and Lee (2000) was always less than 7 percent. The interfacial fracture toughness Γ is much larger than the opening mode fracture toughness Γ_I^c for all delamination lengths, but especially at d=2.5 mm. The interfacial fracture toughness is quite large for d<3.5 mm, compared to the strain energy release rate. Therefore, further propagation of initial delamination (d<3.5 mm) may not occur. The interfacial fracture toughness decreases more rapidly than the strain energy release rate for d>2.5 mm and is relatively smaller than the strain energy release rate when d increases close to 3.5 mm. It can thus be concluded that the growth of an initial delamination leading to the delamination of an entire interface in the PBGA package without moisture will not be expected during solder reflow unless the initial delamination length is pretty large (for example, d>3.5 mm).

- ***Growth of interfacial delamination in the PBGA package with moisture (level 1)***

Fig. 10 shows the stress intensity factors and the phase angle (calculated from Eqs. 2, 3 and 9) at the delamination tip of the PBGA package with moisture (level 1), for different delamination lengths at 220 ℃. Fig. 10 shows that, for d<2.5 mm, the development of initial delamination is mainly dominated by the shearing mode because the K_{II} is close to K_{eff} and the phase angle ψ exceeds 60 degrees. When d>2.5 mm, the K_I increases rapidly, and even exceeds K_{II} (ψ<45degrees) when d increases close to 4 mm, when the fracture mode gradually becomes dominated by the opening mode. This result is reasonable because more normal steam pressure acts on the surfaces of the larger delamination and opens the delamination. Fig. 11 and Tab. 5 show the strain energy release rate (calculated from Eqs. 8 and 17) and the normalized fracture toughness Γ/Γ_I^c (calculated from Eq. 11) at the delamination tip of the PBGA package with moisture (level 1), for different delamination lengths at 220℃. The maximum difference between G calculated from the method proposed by Saitoh, Matsuyama, and Toya (1998) and that proposed by Lau and Lee (2000) is similar to the difference shown in Fig. 9(a) (<7 percent). The strain energy release rate in the case with moisture (level 1) is much higher than in the case without moisture at the larger delamination length due to steam pressure. Note that the strain energy release rate increases rapidly in the case with moisture (level 1) when d increases close to 4 mm, which result is not seen in the case without moisture. The strain energy release rate is quite large for d>1.5 mm, and especially for d>3.5 mm, compared to the interfacial fracture toughness. The strain energy release rate increases rapidly with d while the interfacial fracture toughness decreases close to Γ_I^c. Hence, the growth of an initial delamination leading to the delamination of an entire interface in the PBGA package with moisture (level 1) will be expected during solder reflow. Note that the critical size of an initial delamination required to cause delamination growth in the case with moisture (level 1) is smaller than that required in the case without moisture. Accordingly, the steam pressure loading has a higher potential than the thermal loading to cause delamination of an entire interface during solder reflow.

4 Experimental verification

An experimental procedure referring to the JEDEC (1995) test standard was performed to verify the above analytical results. First, PBGA packages with 256 I/O's of 1.27-mm pitch were prepared and divided into four groups. All samples were inspected prior to the moisture preconditioning for existing delaminations using C-mode scanning acoustic microscopy (C-SAM). All good PBGA packages were dry baked in an oven at 125℃ for 24 hours to remove the residual moisture. Later, three baked groups of packages were placed in an hygrothermal chamber and subjected to three different JEDEC moisture levels as follows.

Level 1: 85℃/85%RH for 168 hours

Level 2: 85℃/60%RH for 168 hours

Level 3: 30℃/60%RH for 192 hours.

After the moisture preconditioning, four groups of PBGA packages were three times subjected to IR reflow. Finally, all PBGA samples were examined again for evidence of delamination or popcorn cracking using C-SAM and an optical microscope. Tab. 6 summarizes the results. The interfacial delaminations occurred only when PBGA packages were subjected to level 1 preconditioning and IR reflow. Fig. 12 shows the C-SAM images of 256 PBGA packages subjected to different moisture preconditionings and IR solder reflow. Delaminations indicated by the large dark area in the image were observed in PBGA packages undergoing level 1 preconditioning and IR reflow. No delamination was observed in PBGA packages under three other environmental conditions. Fig. 13 shows the cross section of the 256 PBGA package subjected to moisture level 1 preconditioning and IR solder reflow. Fig. 13 shows that delamination occurred in the die attach area (see (a)), and between EMC and the die pad and between EMC and the resin of the BT substrate (see (b)). No delamination was observed in other interfaces of the PBGA package. Thus, predicted results correspond well with experimental results. Therefore, the analytical technique for the simulation of delamination growth of a 3-D PBGA package in this paper is viable.

5 Conclusions

The initial location of the possible delamination in the PBGA package under moisture absorption preconditioning and solder reflow was investigated. The fracture parameters such as the stress intensity factor, the strain energy release rate and the phase angle at the delamination tip were calculated to study the growth of initial delamination of PBGA packages with and without moisture. A series of popcorn experiments were performed to verify the analytical results. Conclusions follow.

1. When the PBGA package is subjected to moisture level 1 preconditioning and solder reflow, the delamination initiation at the EMC/die pad interface near the corners of the die and die pad is expected.
2. The shear mode dominates the fracture mode in the growth of delamination for the PBGA package without moisture.
3. Growth of an initial delamination leading to the delamination of an entire interface is not expected

during solder reflow for the PBGA package without moisture,.

4. The shear mode dominates the fracture mode at smaller delamination lengths and the fracture mode gradually becomes dominated by the opening mode as the delamination length increases, for the PBGA package with moisture (level 1).
5. Growth of an initial delamination leading to the delamination of an entire interface is expected during solder reflow for the PBGA package without moisture.
6. The strain energy release rate at the delamination tip for an arbitrary delamination length, calculated from the method proposed by Saitoh et al. (1998) is almost the same as that calculated by the method of Lau and Lee (2000), for PBGA packages with and without moisture.
7. Delaminations only induced in PBGA package subjected to 85℃/85% RH (168 hrs) and IR reflow, are located in the die attach area, between EMC and the die pad and between EMC and the resin of the BT substrate.
8. Predicted results agree well with experimental results. The analytical technique presented in this paper is viable for the simulation of delamination growth of the 3-D PBGA package.

Acknowledgement

The support from National Center for High-performance Computing by providing supercomputer VPP 300 is greatly acknowledged. The authors would like to thank Prof. Meng-Kao Yek for his helpful discussions. The authors would also like to thank Advanced Semiconductor Engineering, Inc. (ASE) and Neopac Semiconductor Corp., Taiwan, R.O.C., for providing respectively PBGA packages and experimental instruments used for the popcorn experiments of PBGA packages.

References

Ahn, S. H.,; Kwon, Y. S. (1995): Popcorn Phenomena in Ball Grid Array Package. *IEEE Transactions on Components, Packaging, and Manufacturing Technology,* Part B, Vol. 18, No. 3, pp. 491-495, June.

Chang, K. C.; Yeh, M. K.; Chiang K. N.: Hygrothermal Stress Analysis of Plastic Ball Grid Array Package During Solder Reflow. sent to *Journal of the Chinese institute of Engineers*.

Choi, Y. T.; Hu, Y. C. (1998): Analysis of Popcorn Phenomenon of PBGA by Computer Simulation. *Industrial Materials,* Vol. 141, pp. 145-152. (in Chinese)

Hawkins, G.; Ganesan, G.; Lewis, G.; Berg, H. (1995): The PBGA: A Systematic Study of Moisture Resistance. *The International of Microcircuits and Electronic Packaging,* Vol. 18, No. 2, pp. 122-132, Second Quarter.

Hong, B. Z.; Su, L. S. (1998): On Thermal Stresses and Reliability of a PBGA Chip Scale Package. *48th Electronic Components and Technology conference,* pp. 503-510.

Hutchinson, J. W.; Suo, Z. (1991): Mixed Mode Cracking in Layered Materials. *Advance in Applied Mechanics,* Academic Press, Vol. 29, PP. 63-91.

JESD22-A112-A. (1995): Test Method A112-A Moisture-Induced Stress Sensitivity for Plastic Surface Mount Devices. JEDEC Standard, Electronic Industries Association, Arlington, VA, pp. 1-9.

Lau, J. H.; Lee, S. W. R. (2000): Temperature-Dependent Popcorning Analysis of Plastic Ball Grid Array Package During Solder Reflow With Fracture Mechanics Method. *Journal of Electronic Packaging,* ASME, Vol. 122, pp. 34-41, March.

Mei, Y. H.; Liu, S. (1995): An Investigation to Popcorning Mechanisms for IC Plastic Packages: Defect Initiation. *Application of Fracture Mechanics in Electronic Packaging and Materials,* ASME, EEP-Vol. 11/MD-Vol. 64, pp. 85-97.

Nguyen, L. T. (1993): Reliability of Post-molded IC Packages. *Journal of Electronic Packaging, ASME,* Vol. 115, pp. 346-355.

Park, Y. B.; Yu, J. (1997): A Fracture Mechanics Analysis of the Popcorn Cracking in the Plastic IC Packages. *IEEE/CPMT Int'l Electronics Manufacturing Technology Symposium*, pp. 12-19.

Rice, J. R. (1988): Elastic Fracture Mechanics Concepts for Interfacial Cracks. *Transactions of the ASME, Journal of Applied Mechanics,* Vol. 55, pp. 98-103.

Saitoh, T.; Matsuyama, H.; Toya, M. (1998): Linear Fracture Mechanics Analysis on Growth of Interfacial Delamination in LSI Plastic Packages under Temperature Cyclic Loading. *IEEE Transactions on Components, Packaging, and Manufacturing Technology*, Part B, Vol. 21, No. 4, pp. 422-427, November.

Shirley, A. G.; McCullen, J. T. (1995): Component Reliability. *45th IEEE Electronic Components and Technology Conference.*

Voleti, S. R.; Chandra, N.; Miller, J. R. (1996): Global-Local Analysis of Large-Scale Composite Structure Using Finite Element Methods. *Computers & Structures*, Vol. 58, No. 3, pp. 453-464.

Yeh, M. K.; Chang, K. C. (1999a): Failure Prediction in Plastic Ball Grid Array Electronic Packaging. *InterPACK'99*, Hawaii, USA.

Yeh, M. K.; Chang K. C. (1999b): Stress Intensity Factor Analysis at Delamination Tip of Plastic Ball Grid Array Package. *Proceedings of the 16th National Conference on Mechanical Engineering, the Chinese Society of Mechanical Engineers*, Hsinchu, Taiwan, R.O.C., Advanced Engineering Technology Volume, pp. 283-290. (in Chinese)

Captions

Table 1 : Material properties of the PBGA package.

Table 2 : Allowable failure stresses at three interfaces.

Table 3 : Maximum failure index at three interfaces.

Table 4 : Strain energy release rate and normalized fracture toughness at different delamination length for the PBGA package without moisture.

Table 5 : Strain energy release rate and normalized fracture toughness at different delamination length for the PBGA package with moisture.

Table 6 : Experimental results of the PBGA package under different loading conditions.

Figure 1 : Schematic of crack tip opening displacements (CTOD).

Figure 2 : (a) Top view (b) bottom view of the PBGA package.

Figure 3 : Cross-sectional dimension of the PBGA package.

Figure 4 : (a)Peeling stress (b) shear stress at the EMC/die pad interface.

Figure 5 : Predicted delamination initiation and assumption of the delamination growth path.

Figure 6 : One-eighth finite element mesh of the 3-D PBGA package with delamination.

Figure 7 : Finite element local mesh near the delamination tip.

Figure 8 : Variations of the stress intensity factor and the phase angle with the delamination length for the PBGA package without moisture.

Figure 9 : Variations of (a) strain energy release rate and (b) normalized fracture toughness with the delamination length for the PBGA package without moisture.

Figure 10 : Variations of the stress intensity factors and the phase angle with the delamination length for

the PBGA package with moisture (level 1).

Figure 11 : Variations of (a) strain energy release rate and (b) normalized fracture toughness with the delamination length for the PBGA package with moisture (level 1).

Figure 12 : C-SAM images of PBGA packages subjected to different moisture preconditionings and IR solder reflow (the large dark area indicates the delamination region).

Figure 13 : Cross section of the PBGA package subjected to moisture level 1 preconditioning and IR solder relow.

Table 1 : Material properties of the PBGA package.

Material	EMC	Die	Die Attach	Solder Mask	Die Pad	BT	Solder Ball
E (GPa)	14.5	162	8.96	3.448	117	26 x,z 11 y	26.447
CTE ($ppm/^{\circ}C$)	13 x,z 50 y	2.3	15	30	16.7	15 x,z 52 y	25.2
ν	0.32	0.28	0.25	0.35	0.34	0.39 xy,yz 0.11 xz	0.36
K ($w/m^{o}C$)	0.84	110	4.5	0.2	389	3	51
c_p ($J/kg^{o}C$)	1884	712	703	1190	385	1190	150
ρ (kg/m^3)	1900	2330	3800	1995	8942	1995	8470

Source: Hong and Su (1998)

Table 2 : Allowable failure stresses at three interfaces.

Interface	Allowable Peeling Stress (MPa)	Allowable Shear stress (MPa)
EMC/Die	68.556	68.556
Die/Die Attach	68.556	68.556
EMC/Die Pad	3.567	3.567

Source: Choi and Hu (1998)

Table 3 : Maximum failure index at three interfaces.

Interface	EMC/Die	Die/Die Attach	EMC/Die Pad
Max. f_d	0.879	0.925	15.132

Table 4 : Strain energy release rate and normalized fracture toughness at different delamination length for the PBGA package without moisture.

Delamination Length (mm)	0.5	1	2.5	3.5	4
G^S (J/m^2)	0.437	1.593	21.444	8.406	8.534
G^L (J/m^2)	0.392	1.428	20.022	7.849	7.999
Γ/Γ_I^c	3.260	3.198	163.922	3.884	3.042

Note: G^S and G^L indicate respectively that G is calculated from Saitoh, Matsuyama, and Toya (1998) and Lau and Lee (2000).

Table 5 : Strain energy release rate and normalized fracture toughness at different delamination length for the PBGA package with moisture (level 1).

Delamination Length (mm)	0.5	1	2.5	3.5	4
G^S (J/m^2)	0.406	0.197	29.554	18.769	38.558
G^L (J/m^2)	0.364	0.176	27.596	17.525	36.002
Γ/Γ_I^c	3.254	10.142	18.638	1.857	1.353

Note: G^S and G^L indicate respectively that G is calculated from Saitoh, Matsuyama, and Toya (1998) and Lau and Lee (2000).

Table 6 : Experimental results of the PBGA package under different loading conditions.

Loading conditions	125 ^oC prebaking 24 hrs + IR solder Reflow	85 ^oC / 85%RH 168 hrs (level 1) + IR solder Reflow	85 ^oC / 60%RH 168 hrs (level 2) + IR Solder Reflow	30 ^oC / 60%RH 192 hrs (level 3) + IR Solder Reflow
Interfacial Delamination	0/3	6/6	0/3	0/4

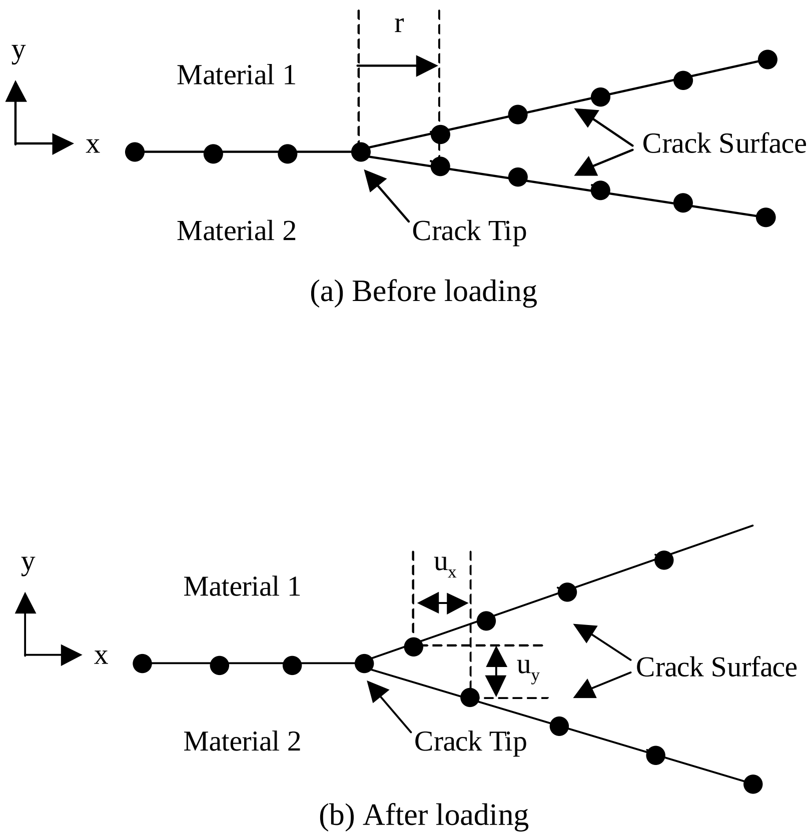

Figure 1 : Schematic of crack tip opening displacements (CTOD).

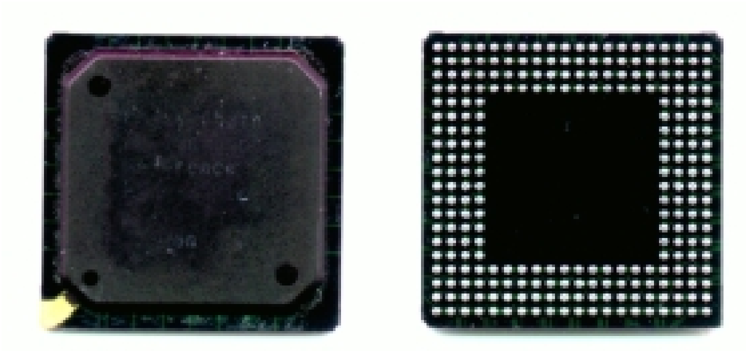

(a) (b)

Figure 2 : (a) Top view (b) bottom view of the PBGA package.

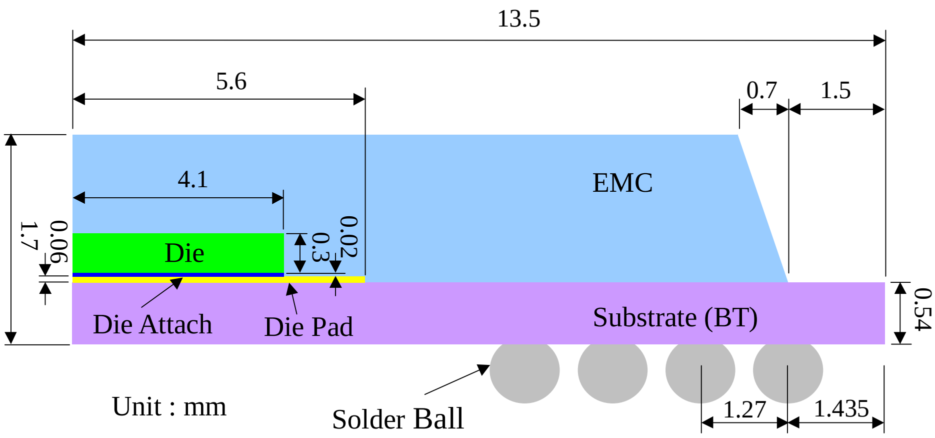

Figure 3 : Cross-sectional dimension of the PBGA package.

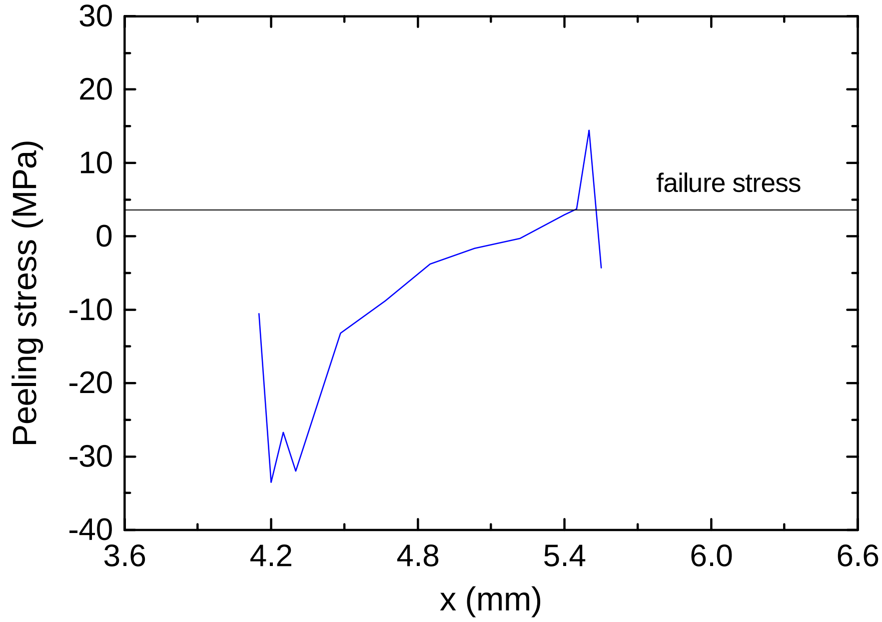

(a)

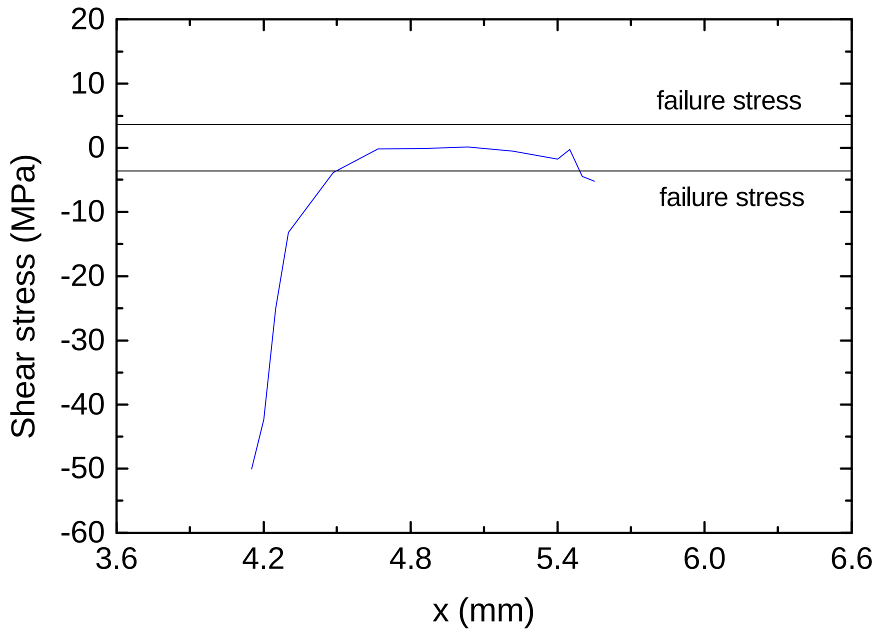

(b)

Figure 4 : (a) Peeling stress (b) shear stress at EMC/die pad interface.

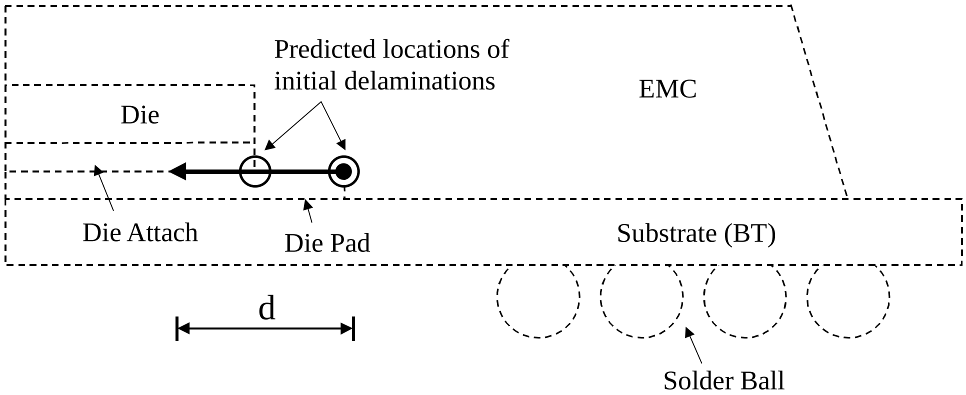

Note: ◀━━● indicates the delamination (the solid circle of arrow indicates the starting point of delamination and the tip of arrow indicates the delamination tip) and d indicates the delamination length

Figure 5 : Predicted delamination initiation and assumption of the delamination growth path.

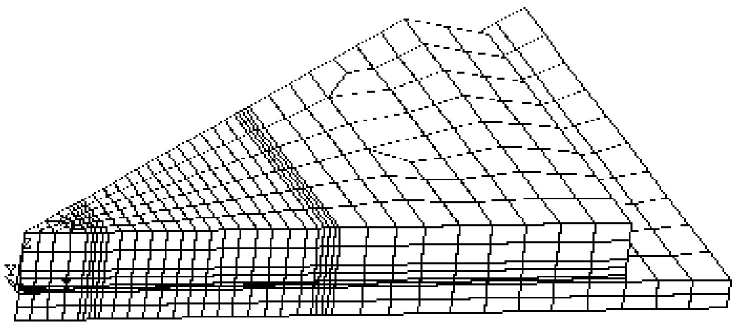

Figure 6 : One-eighth finite element mesh of the 3-D PBGA package with delamination.

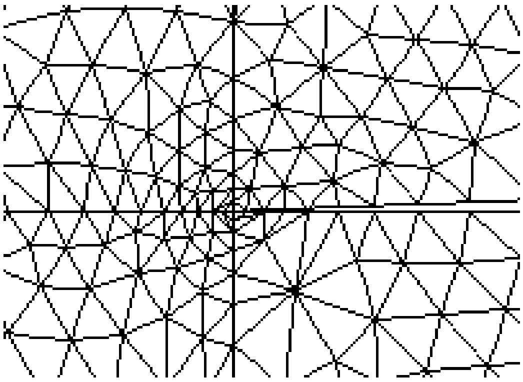

Figure 7 : Finite element local mesh near the delamination tip.

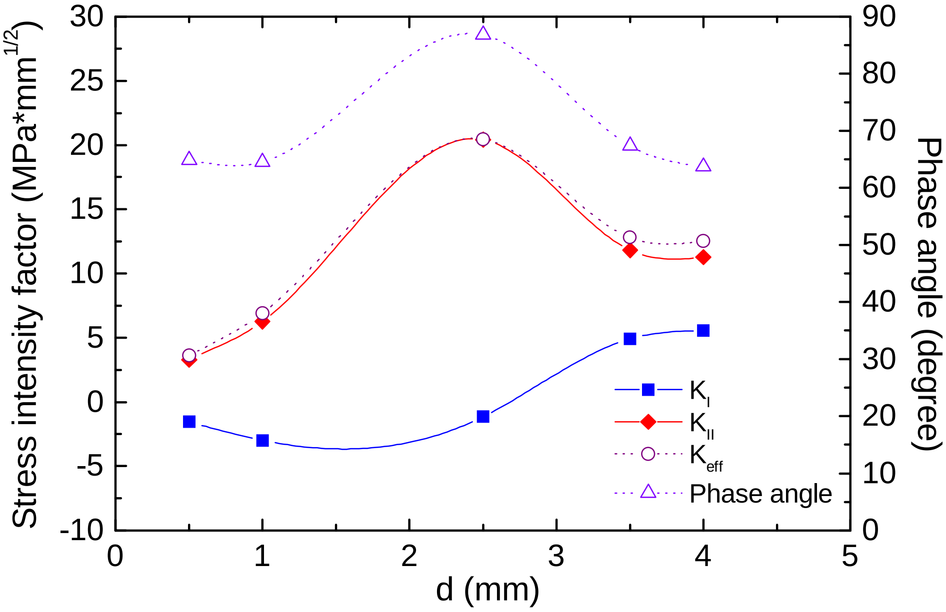

Figure 8 : Variations of the stress intensity factor and the phase angle with the delamination length for the PBGA package without moisture.

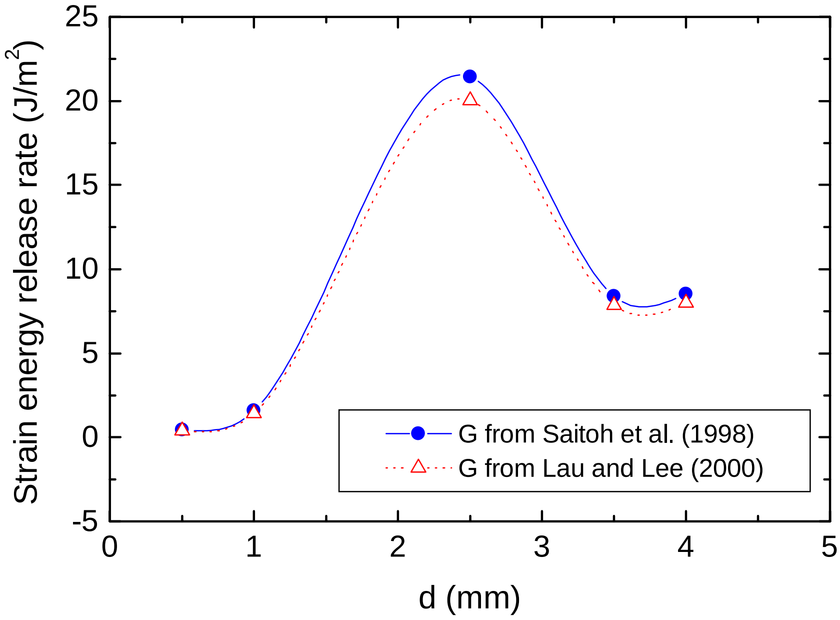

(a)

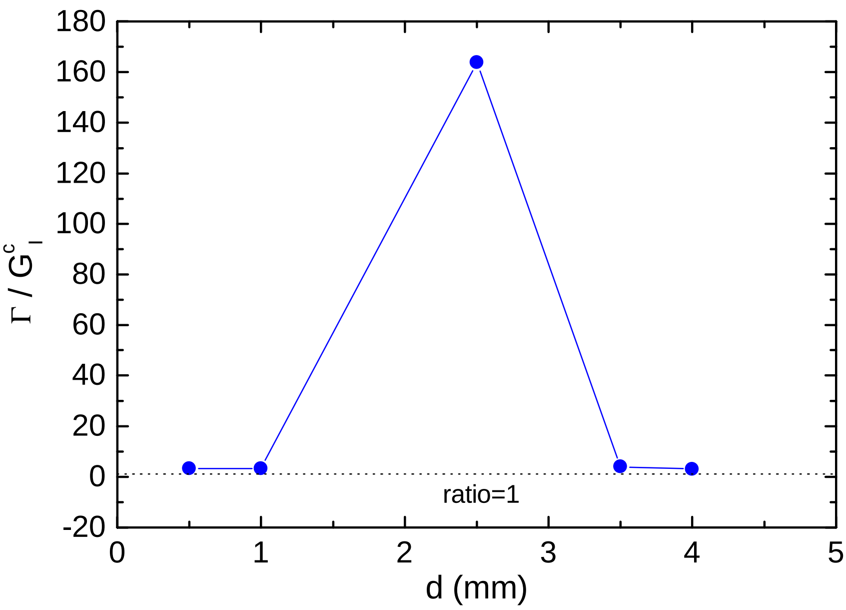

(b)

Figure 9 : Variations of (a) strain energy release rate and (b) normalized fracture toughness with the delamination length for the PBGA package without moisture.

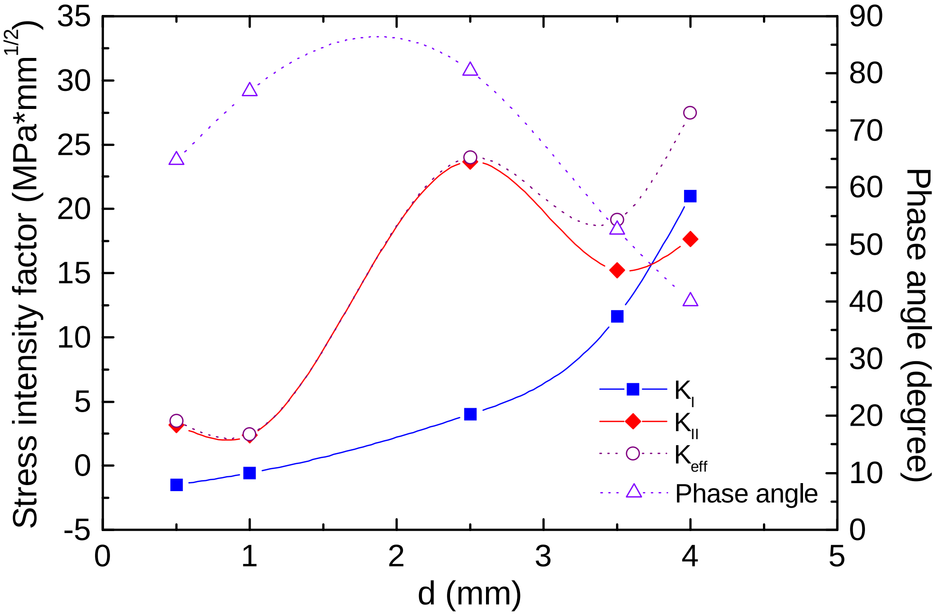

Figure 10 : Variations of the stress intensity factors and the phase angle with the delamination length for the PBGA package with moisture (level 1).

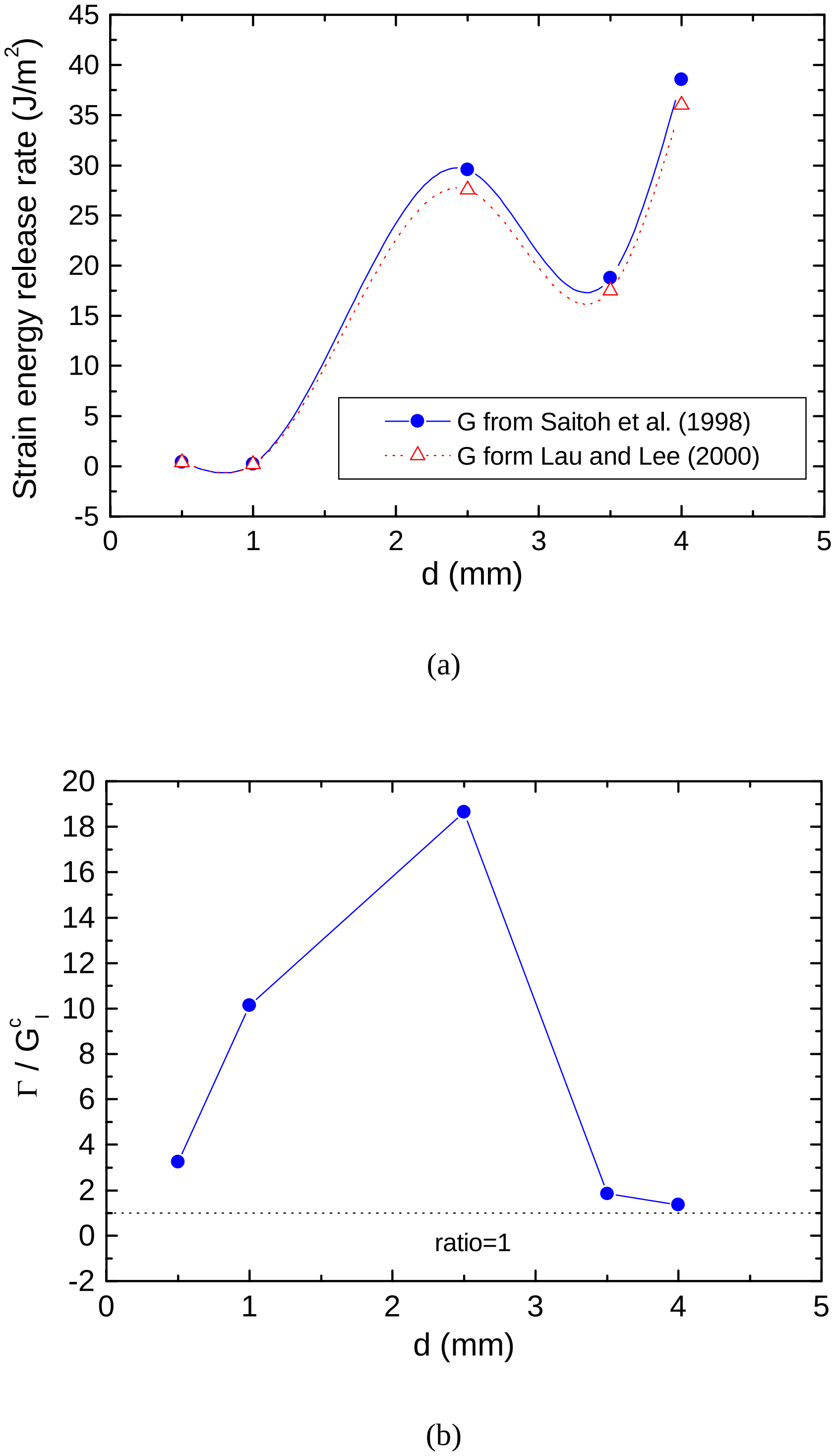

Figure 11 : Variations of (a) strain energy release rate and (b) normalized fracture toughness with the delamination length for the PBGA package with moisture (level 1).

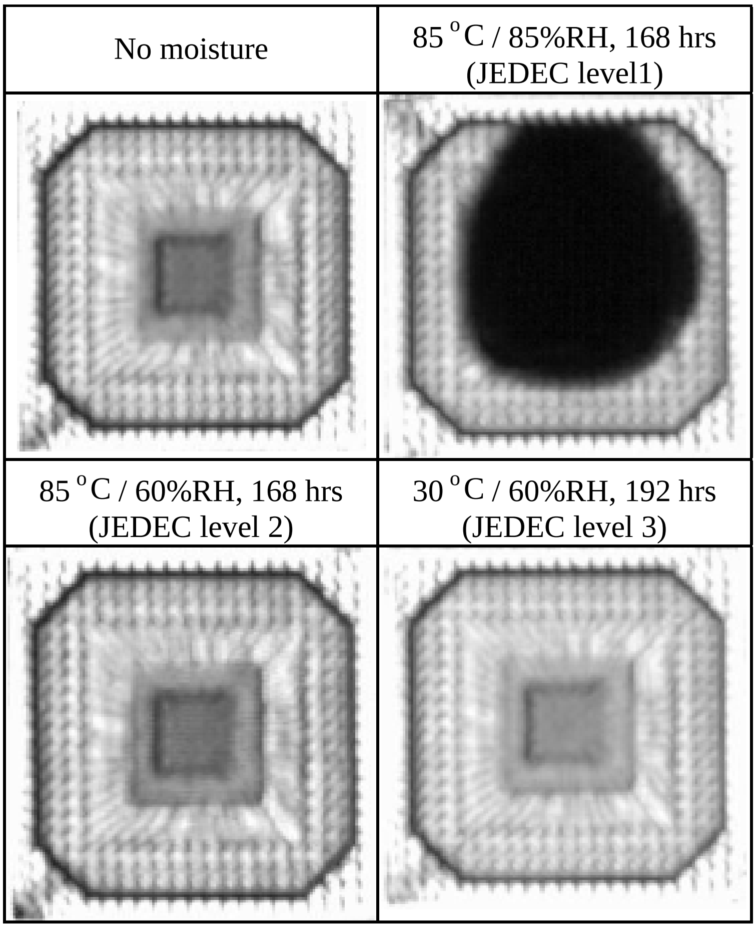

Figure 12 : C-SAM images of PBGA packages subjected to different moisture preconditionings and IR solder reflow (the large dark area indicates the delamination region).

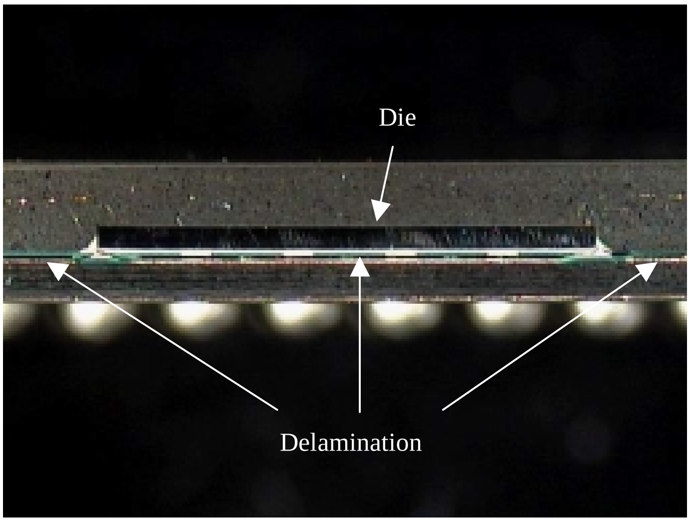

(a)

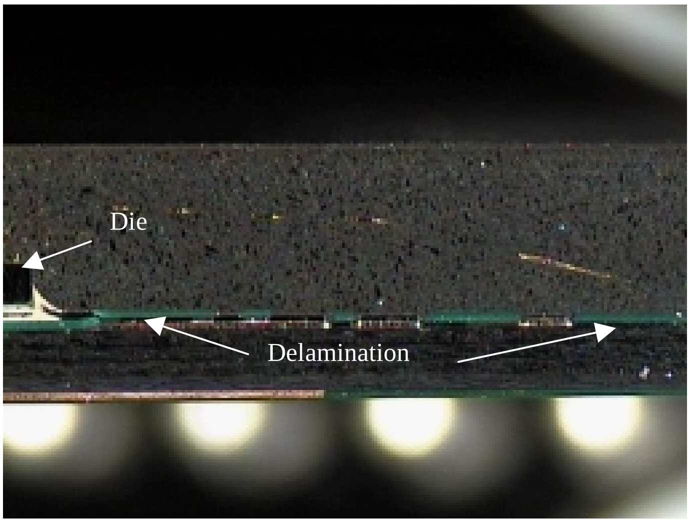

(b)

Figure 13 : Cross section of the PBGA package subjected to moisture level 1 preconditioning and IR solder relow.